Experimental study of the decays of ^{112}Cs and ^{111}Xe

L. Cartegni, C. Mazzocchi, R. Grzywacz, I. G. Darby, S. N. Liddick, K. P. Rykaczewski, J. C. Batchelder, L. Bianco, C. R. Bingham, E. Freeman, C. Goodin, C. J. Gross, A. Guglielmetti, D. T. Joss, S. H. Liu, M. Mazzocco, S. Padgett, R. D. Page, M. M. Rajabali, M. Romoli, P. J. Sapple, J. Thomson, and H. V. Watkins

Phys. Rev. C **85**, 014312 — Published 17 January 2012

DOI: 10.1103/PhysRevC.85.014312

Experimental study of the decays of ^{112}Cs and ^{111}Xe

L. Cartegni,[1] C. Mazzocchi,[2,3] R. Grzywacz,[1,4] I.G. Darby,[1] S.N. Liddick,[1] K.P. Rykaczewski,[4] J.C. Batchelder,[5] L. Bianco,[6] C.R. Bingham,[1,4] E. Freeman,[1] C. Goodin,[7] C.J. Gross,[4] A. Guglielmetti,[2] D.T. Joss,[6] S.H. Liu,[7] M. Mazzocco,[8] S. Padgett,[1] R.D. Page,[6] M.M. Rajabali,[1] M. Romoli,[9] P.J. Sapple,[6] J. Thomson,[6] and H.V. Watkins[6]

[1]Department of Physics and Astronomy, University of Tennessee, Knoxville, Tennessee 37996, USA
[2]Università degli Studi di Milano and INFN, Sez. di Milano, I-20133 Milano, Italy
[3]Faculty of Physics, University of Warsaw, Pl 00-681 Warszawa, Poland
[4]Physics Division, Oak Ridge National Laboratory, Oak Ridge, Tennessee 37831, USA
[5]UNIRIB, Oak Ridge Associated Universities, Oak Ridge, Tennessee 37831, USA
[6]Department of Physics, University of Liverpool, Liverpool, L69 7ZE, United Kingdom
[7]Department of Physics and Astronomy, Vanderbilt University, Nashville, Tennessee 37235, USA
[8]Università degli Studi di Padova and INFN, Sez. di Padova, I-35131 Padova, Italy
[9]INFN, Sez. di Napoli, I-80126 Napoli, Italy

An experiment to search for the alpha decay of ^{112}Cs has been performed at the Holifield Radioactive Ion Beam Facility (HRIBF) at Oak Ridge National Laboratory. The alpha decay of ^{112}Cs was not observed, thus setting the upper limit of the alpha branching ratio at 0.26%. The half-life of ^{112}Cs was measured as $506 \pm 55\,\mu$s. In the same measurement the decay properties of its proton decay daughter ^{111}Xe were also reinvestigated. The newly measured alpha branching ratio for ^{111}Xe is $10.4 \pm 1.9\,\%$. The experimental proton separation energies S_p for odd-Z nuclei above ^{100}Sn were compared to shell model calculations. The calculated proton separation energies for ^{103}Sb and ^{102}Sb point to half-lives of the order of 10 ps and 1 ns, respectively.

I. INTRODUCTION

Tin-100 is to date the heaviest known doubly-magic nucleus with the same number of protons and neutrons. This renders the region of the nuclidic chart above ^{100}Sn particularly interesting for probing nuclear structure, since protons and neutrons outside the closed shells occupy orbitals with the same quantum numbers. It is expected that some of these nuclei may have an unusually large reduced alpha-decay width, resulting in the so-called superallowed alpha decay [1–3]. Another interesting feature of this portion of the chart of nuclei is the presence of the proton drip-line. These features give rise to an island of alpha and proton decay between Z=52 and 56, just above ^{100}Sn. Both alpha and proton decay may become possible for the same nucleus and compete with each other [4–6].

So far the only nuclide in this region that has been identified as both an alpha and proton emitter is ^{109}I [6]. By measuring decay Q-values and relating them to isotopes whose mass is measured, it is possible to deduce the mass of nuclei far from stability at the limit of nuclear existence, with an accuracy of the order of 10 keV. This method allowed the proton separation energy S_p of ^{105}Sb to be determined from the alpha decay Q-value (Q_α) of ^{109}I [6].

Among the candidates for having both alpha and proton decay branches, we chose to investigate $^{112}_{55}$Cs$_{57}$. It is a known proton emitter; its half-life $T_{\frac{1}{2}} = 500 \pm 100\,\mu$s and proton energy 807±7 keV were determined from the observation of about 20 decay events [7]. In analogy with the approach followed for the investigation of ^{109}I alpha decay [6], the measurement of the Q_α value for ^{112}Cs would determine indirectly the proton separation energies of ^{104}Sb and ^{108}I, as shown in Figure 1. An upper limit for $Q_p(^{108}\mathrm{I})$, which implies an upper limit for $Q_p(^{104}\mathrm{Sb})$, was deduced in [5]. Adopting those upper limits, a lower limit of 3.83 MeV can be estimated for the ^{112}Cs Q_α value.

The daughter of ^{112}Cs proton decay, ^{111}Xe, has a half-life of 0.74 ± 0.20 s and decays with the emission of 3580 ± 30 keV and 3480 ± 30 keV alpha particles [8]. It has been established that these transitions are due to the ground state of ^{111}Xe decaying to the ground state or to the first excited state of ^{107}Te, respectively [9]. The alpha branching ratio is $8^{+8}_{-5}\,\%$ [5].

The properties of these nuclei are also of interest to stellar nucleosynthesis studies. The astrophysical rapid proton capture (rp-) process was expected to terminate in a loop around neutron-deficient Sn-Sb-Te isotopes, close to ^{100}Sn [10]. The network calculations used to determine the path followed by the rp-process require as input parameters the particle-separation energies of the nuclei involved. Reaction and capture rates depend strongly on Q-values [11]. Since theoretical mass-models are not sufficiently reliable in this region of the nuclidic chart, their experimental determination is critical. Recently, the proton separation energy of ^{106}Sb was determined experimentally [12], the measured values indicating that the rp-process does not terminate in a loop as originally thought, but it simply dies out. Nevertheless, the determination of the proton separation energies of its more exotic neighbouring nuclei, including ^{104}Sb, is still important in order to rule out completely the existence of the Sn-Sb-Te loop, which could survive through proton capture on ^{103}Sn, if ^{104}Sb is more proton bound than predicted [6].

Here we report on the search for the weak alpha-decay branch of ^{112}Cs and the reinvestigated decay of its daugh-

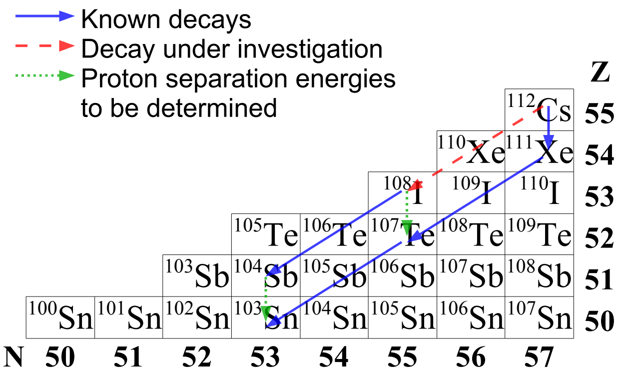

FIG. 1: (Color online) Portion of the nuclide chart above ^{100}Sn. The arrows show decay chains starting at ^{112}Cs.

ter and granddaughter nuclei, ^{111}Xe and ^{107}Te.

II. EXPERIMENT

The experiment was performed at the Holifield Radioactive Ion Beam Facility (HRIBF) at Oak Ridge National Laboratory. A beam of ^{58}Ni at 250 MeV impinged on a ^{58}Ni target (300 μg/cm^2 thick), producing ^{112}Cs ions via the fusion-evaporation reaction $^{58}\mathrm{Ni}\left(^{58}\mathrm{Ni}, \mathrm{p3n}\right)^{112}\mathrm{Cs}$.

The target was mounted on a rotating support, so that it could sustain higher beam intensities with respect to a stationary target. Typical beam intensities ranged between 20 and 40 particle·nA. The recoiling reaction products were separated by the Recoil Mass Spectrometer (RMS) [13] according to their mass-to-charge ratio A/Q. The charge states 30+ and 31+ were selected for ^{112}Cs ions. At the focal plane the separated recoils passed through a Microchannel Plate (MCP) detector [14] that provided a two-dimensional image of the position of the ions arriving at the focal plane.

The recoils were then implanted into a Double-sided Silicon Strip Detector (DSSD) of 65 μm thickness, segmented in 40 horizontal strips in the front and 40 vertical strips in the back. It detected the incoming ions and measured their subsequent decays. The typical ion implantation rate was of the order of 1 ion per second per pixel. The energy of the recoil ions at the focal plane of the RMS was of the order of 100 MeV, while the energy of the decay products ranged between 0.8 MeV for protons and several MeV for alpha and beta-delayed alpha particles and protons. Thin layers of aluminum and mylar (308 and 354 μg/cm^2 thick, respectively) were placed in front of the DSSD as degraders, to reduce the energy of incoming ions to within the range of the DSSD electronics. The average energy of recoil ions after the degraders was 74 MeV. The detection setup also included a series of veto detectors, that suppressed particles escaping the DSSD detector with good efficiency [15]: upstream a box consisting of 4 silicon detectors (Si-box) surrounded the DSSD, while a 5 mm-thick Si(Li) detector was placed just behind it in close geometry.

Data from all detectors were collected by digital signal processing electronics [16]. Each event was time-stamped and registered with its amplitude. In the offline software analysis of the data, decay events were correlated in time and space with the implanted ions.

III. RESULTS AND DISCUSSION

A. Decay of ^{112}Cs

The search for alpha particles emitted by ^{112}Cs was conducted by looking for the alpha-decay chain $^{112}\mathrm{Cs} \rightarrow {}^{108}\mathrm{I} \rightarrow {}^{104}\mathrm{Sb}$. This was implemented by inspecting the sequence of implant-decay-decay events within one pixel, in anticoincidence with the veto detectors to suppress escape events. Moreover, a time correlation window of 100 ms between the first and the second decay event could be imposed ($\mathrm{T}_{\frac{1}{2}}(^{108}\mathrm{I}) = 36 \pm 6$ ms [5]).

Figure 2 shows the spectrum of first generation decay events collected in 120 hours of measurement. The lower energy peak corresponds to the protons emitted by ^{109}I and ^{112}Cs (811 ± 5 keV [17] and 807 ± 7 keV [7], respectively) that cannot be resolved, while the higher energy peak corresponds to the protons emitted by ^{113}Cs ($\mathrm{E}_p = 960 \pm 3$ keV [18], $T_{\frac{1}{2}} = 18.3 \pm 0.3\,\mu$s [19]). Both ^{109}I and ^{113}Cs are present in the beam as either charge-state contaminants or tail-of-the-recoil-distribution contaminants. The amount of ^{109}I present in the beam was determined by analysing the time distribution of the ^{109}I and ^{112}Cs protons, since their half-lives differ by a factor of about 5. Figure 3 shows the proton decay of ^{112}Cs and ^{109}I. The exponential curve describes the decay of both nuclei, with the half-life of ^{109}I being $93.5 \pm 0.3\,\mu$s [6]. This time decay curve was fitted to the data with a Poisson maximum log-likelihood metod, which has been shown to give better results than chi-square methods for counting experiments [20]. From these data the half-life of ^{112}Cs could be determined with higher precision to be $506 \pm 55\,\mu$s.

Figure 4 shows the decay-decay correlated events. Two known decay chains can be identified:

$^{112}\mathrm{Xe} \rightarrow {}^{108}\mathrm{Te} \rightarrow {}^{104}\mathrm{Sn}$

$^{111}\mathrm{Xe} \rightarrow {}^{107}\mathrm{Te} \rightarrow {}^{103}\mathrm{Sn}$

The alpha decay of ^{111}Xe is preceded by the proton decay of ^{112}Cs, which may be undetected if it occurs within 100 μs of an ion implantation. Some of the alpha decays of ^{111}Xe thus appear in this figure as first generation decays, while they are actually second generation decays.

The alpha decay of ^{112}Cs would be expected to have a Q value of at least 3.83 MeV, as noted in the Introduction, and to be followed by the alpha decay of ^{108}I

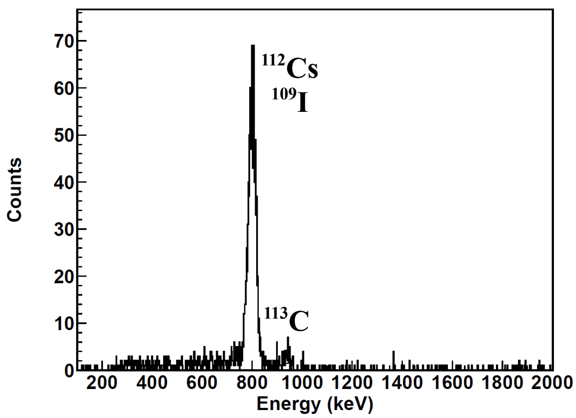

FIG. 2: Portion of the energy spectrum of decay events following the implantation of an ion in the same pixel of the detector. This spectrum shows decays within 5 ms of a recoil.

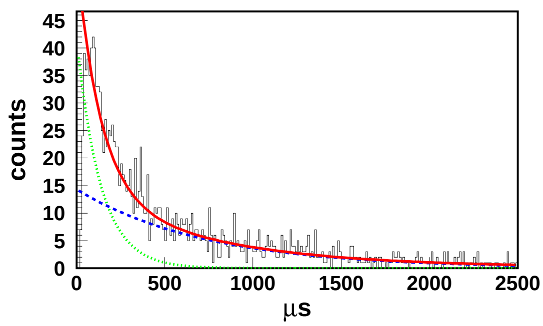

FIG. 3: (Color online) Proton decay of ^{109}I and ^{112}Cs, with the time decay curve used to determine the half-life of ^{112}Cs. The dashed line represents the decay of ^{112}Cs, and the dotted line represents the decay of ^{109}I.

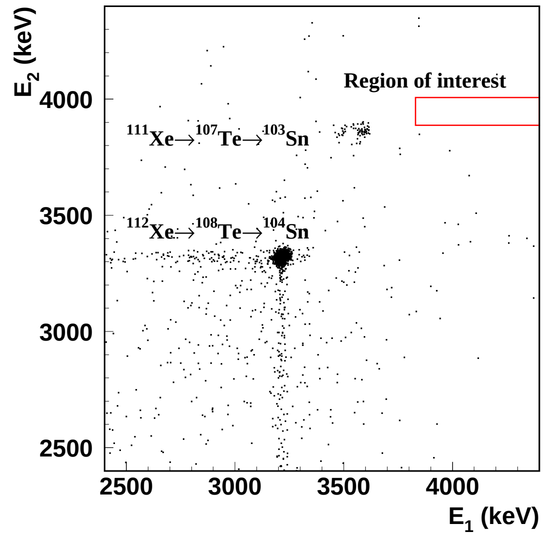

FIG. 4: Decay-decay correlated events: the energy of the first decay event detected after ion implantation is on the horizontal axis, while the energy of the second decay event in the same DSSD pixel is on the vertical axis. The box shows where alpha decay of ^{112}Cs, correlated to alpha decay of ^{108}I (3947 ± 5 keV [5]), would be expected.

TABLE I: Summary of the newly estimated Q_p and Q_α values.

Nucleus	Q_p (MeV)	Q_α (MeV)
^{104}Sb	0.15–0.52	
^{108}I	0.24–0.60	
^{112}Cs		3.83–4.21

with energy 3947 ± 5 keV, corresponding to a Q value of 4099 ± 5 keV [5]. The alpha decay of ^{112}Cs was not observed in these measurements, therefore only an upper limit to the branching ratio for α decay of ^{112}Cs could be inferred. We took into account the alpha branching ratio of ^{108}I (91^{+9}_{-14} % [5]) and the detection efficiency for alphas (83(2) % at 3.83 MeV). The efficiency of the DSSD is calculated from the depth of ion implantation and the range of emitted particles in silicon and tested with a GEANT4 simulation. Using Poisson statistical analysis, we could establish an upper limit of 0.53% for the alpha branching ratio of ^{112}Cs, with 90% confidence level.

In order to estimate the $Q_\alpha$value for ^{112}Cs from the available information, an assumption had to be made. Since away from the Z=50 shell closure, at Z=53, 55, shape deformation is present (of the order of $\beta = 0.1$ for ^{112}Cs [21]), the reduced α-decay width [22] of ^{114}Cs was assumed for ^{112}Cs, i.e. $\delta^2 = 0.072^{+0.048}_{-0.028}$ MeV [23, 24]. In this approximate way the deformation of ^{112}Cs is taken into account: using the reduced α-decay width for the neighbour ^{114}Cs and δ^2 analysis in the spherical approach, we assume a similar potential tunnelled by the alpha particle for the decay of the two neighboring odd-odd cesium isotopes. Under this ansatz the α branching ratio can be calculated as a function of the Q_α value for l=0 and l=2, as shown in Figure 5. We can therefore infer an upper limit to the Q_α value for ^{112}Cs of 4.21 MeV, as indicated by the vertical dashed line in Figure 5.

The new upper limit on $Q_\alpha\left(^{112}\text{Cs}\right)$ implies lower limits on the Q_p values for ^{104}Sb and ^{108}I of 0.15 MeV and 0.24 MeV, respectively. In Figure 6 the Q_p values for the odd-Z cesium, iodine and antimony isotopes are plotted. An upper limit for $Q_p(^{108}\text{I})$, which implies an upper limit for $Q_p(^{104}\text{Sb})$, was deduced in [5]. This constrains the Q_p values to the energy windows $0.15\,\text{MeV} \leq Q_p(^{104}\text{Sb}) \leq 0.52\,\text{MeV}$ and $0.24\,\text{MeV} \leq Q_p(^{108}\text{I}) \leq 0.60\,\text{MeV}$, as shown by the boxes in Figure 6. These new estimated Q values are also summarized in Table I.

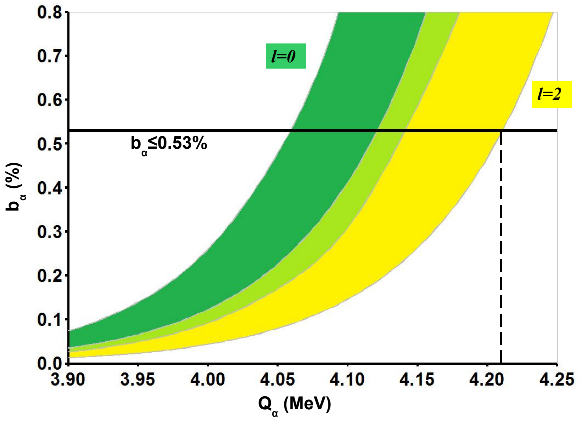

FIG. 5: (Color online) Alpha branching ratio of ^{112}Cs as a function of its Q_α-value. The green (dark) and the yellow (light) bands represent the value with error bars calculated for l=0 and l=2 respectively. The horizontal line shows the measured upper limit for the alpha branching ratio. The dashed vertical line shows the estimated upper limit for the Q_α value. See text for details.

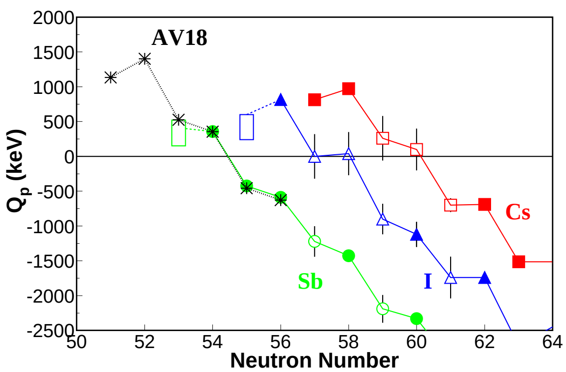

FIG. 6: (Color online) Q_p values for neutron-deficient Sb (Z=51), I (Z=53) and Cs (Z=55) isotopes. Full symbols represent measured values [17] while open symbols represent extrapolations [25]. The boxes represent the energy windows expected for the proton separation energies of ^{104}Sb and ^{108}I ([5] and present work). The symbols connected by the dotted line represent shell model calculations. See text for details.

B. Decay of ^{111}Xe

With this experiment it was also possible to gather information on ^{111}Xe, produced by the proton decay of ^{112}Cs, and its daughter ^{107}Te. In particular, the alpha decay chain ^{111}Xe $\rightarrow$ ^{107}Te $\rightarrow$ ^{103}Sn was studied. Both ^{111}Xe and ^{107}Te are alpha and beta emitters. Their alpha branching ratios are known with low precision, their respective values being $8^{+8}_{-5}\,\%$ [5] and $70 \pm 30\,\%$ [23].

The beta-decay partial half-life of ^{107}Te was calculated in [26] as 0.8994 s. It can also be estimated on the basis of systematics of beta-decay partial half-lives for tellurium isotopes. Figure 7 shows the trend of these values as a

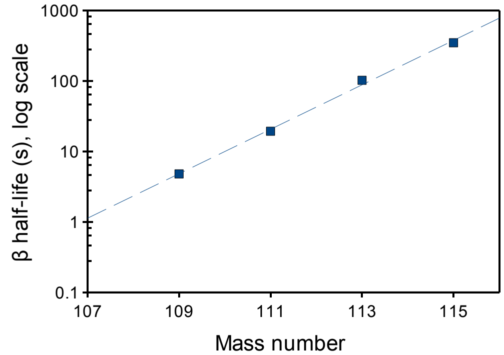

FIG. 7: Partial beta half-life T_β for odd-A tellurium isotopes [27–30] as a function of the mass number A. The straight dashed line represents a linear fit on $ln(T_\beta)$, used to estimate the beta half-life of ^{107}Te.

function of the mass number A, from ^{109}Te to ^{115}Te [27–30]. With a linear regression on $ln(T_\beta)$, the beta-decay partial half-life of ^{107}Te can be estimated to be $1.1 \pm 0.1\,s$. This value, obtained with a simple extrapolation, is in agreement with the value calculated in [26]. Using 3.1 ± 0.1 ms as the total half-life [5], the beta branching ratio for ^{107}Te is calculated to be 0.29(3) %. Its alpha branching ratio is therefore larger than 99.7 %.

In order to determine the alpha branching ratio for ^{111}Xe, the number of ^{111}Xe nuclei needs to be known. This can be directly inferred from the number of protons from the decay of ^{112}Cs, corrected for the detection efficiency for ^{112}Cs protons (97(3) %). The alpha branching ratio of ^{111}Xe can be determined by taking into account the number of ^{111}Xe nuclei, the number of ^{107}Te alpha decays, the detector's efficiency for ^{107}Te alphas (84(2) %), and the newly estimated alpha branching ratio of ^{107}Te. The result is $b_\alpha(^{111}\mathrm{Xe}) = 10.4 \pm 1.9\,\%$, much more accurate than the earlier value of $8^{+8}_{-5}\,\%$ [5].

Figure 8 shows the two alpha transitions from the decay of ^{111}Xe. This observation of fine structure in the alpha decay of ^{111}Xe leads also to an improved determination of the relative branching ratios: 76(5) % of the alpha decays of ^{111}Xe proceed to the ground state of ^{107}Te. This is consistent with the previous result of 69(7) % [23].

The results described so far have been utilized to determine the reduced alpha-decay width for the relevant transitions with improved accuracy, see Table II.

IV. ODD-EVEN EFFECT AND THEORETICAL CALCULATIONS

Pairing forces are manifested in a very particular way through the odd-even effect observed in the proton-separation energies as is shown in Figure 6.

This effect has been observed directly in the proton

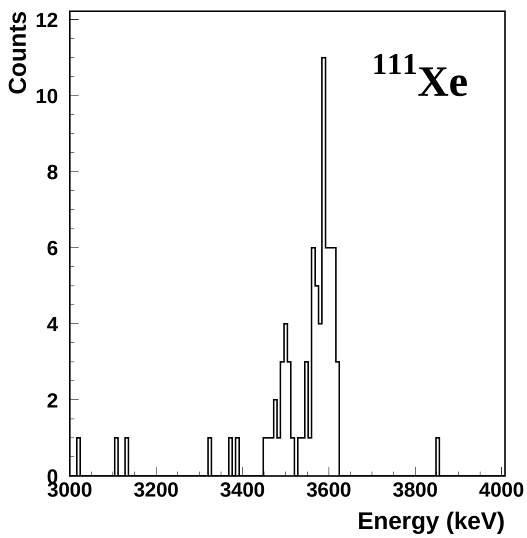

FIG. 8: Energy spectrum of the alpha decay of ^{111}Xe. These decay events are selected by requiring that the next decay in the same DSSD pixel belongs to ^{107}Te. Both the ^{111}Xe alpha transitions are present in the spectrum.

TABLE II: Summary of alpha decay properties of ^{111}Xe and ^{107}Te: energy (E_α), branching ratio (b_α), reduced alpha-decay width (δ^2) and reduced alpha-decay width relative to ^{212}Po (W_α). See text for details.

Nucleus	E_α (MeV)	b_α (%)	δ^2 (MeV)	W_α
^{111}Xe	3582 ± 10 [31]	7.9 ± 1.5	$0.054^{+0.02}_{-0.07}$	$0.78^{+0.11}_{-0.10}$
	3500 ± 15 [32]	2.5 ± 1.7	$0.028^{+0.08}_{-0.04}$	$0.39^{+0.06}_{-0.05}$
^{107}Te	3862 ± 5 [7]	≥ 99.7	$0.14^{+0.02}_{-0.01}$	$2.06^{+0.15}_{-0.14}$

decay for the ^{113}Cs and ^{112}Cs pair [7] as well as for the ^{141}Ho and ^{140}Ho pair [33]. For other pairs of proton emitters like ^{151}Lu and ^{150}Lu [34], and the corresponding low-spin proton emitting isomers ^{151m}Lu [35] and ^{150m}Lu [36] the more exotic odd-odd nucleus has nearly the same proton decay energy as its odd-even less exotic partner. The information on the odd-Z isotopes gathered near ^{100}Sn shows a strong staggering of the proton separation energy, such that for Cs and I the odd-odd emitters have smaller decay energy than their neighbors. This effect seems to be stronger beyond the drip line.

The data points for the antimony (Z=51) isotopes with one proton outside the closed shell are of particular importance because they can be compared to shell model calculations. In this case we have used the same shell model calculations as employed in the ^{105}Te decay study [3] which are derived from nucleon scattering potentials [37]. The nucleon-nucleon potential AV18 [38] was used.

In order to obtain proton separation energies, binding energies have been calculated for the series of Sn and Sb isotopes. This approach is valid locally, where the variations of the binding energy from the nuclear size are small compared to the pairing effects. We have also normalized the proton separation energies to the measured value for ^{105}Sb. The agreement between the known data points for $A > 105$ is very good, thus we assume that this calculation may well describe also the properties of ^{104}Sb, where the theoretical prediction ($Q_p = 0.5(1)$ MeV) is consistent with the observed limit ($Q_p < 0.520$ MeV) within the accuracy of the shell model.

Interesting conclusions can be therefore drawn on the stability of the ^{103}Sb and ^{102}Sb. The odd-even effect leads to ^{103}Sb being a very unstable nucleus, with a predicted Q_p value of 1.4 MeV. The lifetime of such a system is expected to be in the 10 ps range for l=2 emission. This is consistent with the experimental data obtained in [39], where the lifetime limit of this nucleus was established to be smaller than 50 ns. A rather steep drop of Q_p for ^{102}Sb may provide a very intriguing possibility that this nucleus might be a longer lived proton emitter. Here the strong p-n interaction produces a large effect in Sb binding energy, and significant lowering of the Q_p is expected with respect to ^{103}Sb. This particular calculation predicts the Q_p-value to be about 1.13 MeV. The l=2 proton emission leads to a lifetime in the 1 ns range, which is very short and makes the observation in fragmentation reactions using standard techniques impossible. Presently we cannot extend the shell model calculation to the isotopes of iodine and cesium, due to the very large model space.

V. SUMMARY

In this work we present a new measurement of the half-life of ^{112}Cs, which is $506 \pm 55\,\mu$s. The attempt to observe the alpha decay of ^{112}Cs for the first time was not successful, but it allowed an upper limit of 0.26% for its alpha branching ratio to be set. With this result, and assuming that ^{112}Cs has the same reduced alpha-decay width as ^{114}Cs, a new upper limit for the Q_α value of ^{112}Cs and new lower limits for the Q_p values of ^{104}Sb and ^{108}I were deduced. We also present a new measurement of the alpha branching ratio of ^{111}Xe. We have compared the available information on proton emission with shell model calculations, finding very good agreement between observed and predicted proton decay energies. Predictions for proton emission from the more exotic ^{103}Sb and ^{102}Sb have also been made.

Acknowledgments

This research is supported by the Office of Nuclear Physics, US Department of Energy and US DOE grants DE-FG02-96ER40983 and DE-AC05-00OR22725. It is supported in part by the National Nuclear Security Administration under the Stewardship Science Academic Alliances program through DOE Cooperative Agreement DE-FG52-08NA28552, the NNSA through DOE Cooperative Agreement DE-FC03-03NA00143, the UNIRIB Consortium and the U.K. Science and Technology Facilities Council.

[1] R. D. Macfarlane and A. Siivola, Phys. Rev. Lett. **14**, 114 (1965).
[2] S. N. Liddick, R. Grzywacz, C. Mazzocchi, R. D. Page, K. P. Rykaczewski, J. C. Batchelder, C. R. Bingham, I. G. Darby, G. Drafta, C. Goodin, et al., Phys. Rev. Lett. **97**, 082501 (2006).
[3] I. G. Darby, R. K. Grzywacz, J. C. Batchelder, C. R. Bingham, L. Cartegni, C. J. Gross, M. Hjorth-Jensen, D. T. Joss, S. N. Liddick, W. Nazarewicz, et al., Phys. Rev. Lett. **105**, 162502 (2010).
[4] R. Kirchner, O. Klepper, G. Nyman, W. Reisdorf, E. Roeckl, D. Schardt, N. Kaffrell, P. Peuser, and K. Schneeweiss, Nucl. Inst. and Meth. in Phys. Research B **70**, 150 (1977).
[5] R. D. Page, P. J. Woods, R. A. Cunningham, T. Davinson, N. J. Davis, A. N. James, K. Livingston, P. J. Sellin, and A. C. Shotter, Phys. Rev. C **49**, 3312 (1994).
[6] C. Mazzocchi, R. Grzywacz, S. N. Liddick, K. P. Rykaczewski, H. Schatz, J. C. Batchelder, C. R. Bingham, C. J. Gross, J. H. Hamilton, J. K. Hwang, et al., Phys. Rev. Lett. **98**, 212501 (2007).
[7] R. D. Page, P. J. Woods, R. A. Cunningham, T. Davinson, N. J. Davis, A. N. James, K. Livingston, P. J. Sellin, and A. C. Shotter, Phys. Rev. Lett. **72**, 1798 (1994).
[8] D. Schardt, T. Batsch, R. Kirchner, O. Klepper, W. Kurcewicz, E. Roeckl, and P. Tidemand-Petersson, Nucl. Phys. A **368**, 153 (1981).
[9] B. Hadinia, B. Cederwall, K. Lagergren, J. Blomqvist, T. Back, S. Eeckhaudt, T. Grahn, P. Greenlees, A. Johnson, D. T. Joss, et al., Phys. Rev. C **70** (2004).
[10] H. Schatz, A. Aprahamian, V. Barnard, L. Bildsten, A. Cumming, M. Ouellette, T. Rauscher, F.-K. Thielemann, and M. Wiescher, Phys. Rev. Lett. **86**, 3471 (2001).
[11] H. Schatz, A. Aprahamian, J. Grres, M. Wiescher, T. Rauscher, J. F. Rembges, F. K. Thielemann, B. Pfeiffer, P. Mller, K. L. Kratz, et al., Phys. Rep. **294**, 167 (1998), ISSN 0370-1573.
[12] V.-V. Elomaa, G. K. Vorobjev, A. Kankainen, L. Batist, S. Eliseev, T. Eronen, J. Hakala, A. Jokinen, I. D. Moore, Y. N. Novikov, et al., Phys. Rev. Lett. **102**, 252501 (2009).
[13] C. J. Gross, T. N. Ginter, D. Shapira, W. T. Milner, J. W. McConnell, A. N. James, J. W. Johnson, J. Mas, P. F. Mantica, R. L. Auble, et al., Nucl. Instr. and Meth. in Phys. Research A **450**, 12 (2000).
[14] D. Shapira, T. A. Lewis, and L. D. Hulett, Nucl. Instr. and Meth. in Phys. Research A **454**, 409 (2000).
[15] M. Karny, K. P. Rykaczewski, R. K. Grzywacz, J. C. Batchelder, C. R. Bingham, C. Goodin, C. J. Gross, J. H. Hamilton, A. Korgul, W. Królas, et al., Phys. Lett. B **664**, 52 (2008).
[16] R. Grzywacz, Nucl. Instr. and Meth. in Phys. Research B **204**, 649 (2003).
[17] B. Blank and M. Borge, Progress in Particle and Nuclear Physics **60**, 403 (2008).
[18] S. Hofmann, Radiochim. Acta **70/71**, 93 (1995).
[19] C. J. Gross, Y. A. Akovali, C. Baktash, J. C. Batchelder, C. R. Bingham, M. P. Carpenter, C. N. Davids, T. Davinson, D. Ellis, A. Galindo-Uribarri, et al., AIP Conference Proceedings **455**, 444 (1998).
[20] T. Hauschild and M. Jentschel, Nucl. Inst. and Meth. in Phys. Research A **457**, 384 (2001).
[21] L. S. Ferreira and E. Maglione, Phys. Rev. Lett. **86**, 1721 (2001).
[22] J. O. Rasmussen, Phys. Rev. **113**, 1593 (1959).
[23] D. Schardt, R. Kirchner, O. Klepper, W. Reisdorf, E. Roeckl, and P. Tidemand-Petterson, Nucl. Phys. A **326**, 65 (1979).
[24] E. Roeckl, G. M. Gowdy, R. Kirchner, O. Klepper, A. Piotrowski, A. Płochocki, W. Reisdorf, P. Tidemand-Petersson, J. Żylicz, D. Schardt, et al., Zeitschrift fur Physik A **294**, 221 (1980).
[25] G. Audi, O. Bersillon, J. Blachot, and A. H. Wapstra, Nucl. Phys. A **729**, 128 (2003).
[26] P. Möller, J. R. Nix, and K. Kratz, Atomic Data and Nuclear Data Tables **66**, 131 (1997).
[27] J. Blachot, Nuclear Data Sheets **107**, 355 (2006).
[28] J. Blachot, Nuclear Data Sheets **110**, 1239 (2009).
[29] J. Blachot, Nuclear Data Sheets **104**, 791 (2005).
[30] J. Blachot, Nuclear Data Sheets **104**, 967 (2005).
[31] F. Heine, T. Faestermann, A. Gillitzer, J. Homolka, M. Köpf, and W. Wagner, Zeitschrift für Physik A Hadrons and Nuclei **340**, 225 (1991).
[32] F. Heine, T. Faestermann, A. Gillitzer, and H. J. Körner, in *Proceedings of the 6th Conference on Nuclei Far From Stability and the 9th International Conference on Atomic Masses and Fundamental Constants* (1992), p. 331.
[33] K. Rykaczewski, J. C. Batchelder, C. R. Bingham, T. Davinson, T. N. Ginter, C. J. Gross, R. Grzywacz, M. Karny, B. D. MacDonald, J. F. Mas, et al., Phys. Rev. C **60**, 011301 (1999).
[34] P. J. Sellin, P. J. Woods, T. Davinson, N. J. Davis, K. Livingston, R. D. Page, A. C. Shotter, S. Hofmann, and A. N. James, Phys. Rev. C **47**, 1933 (1993).
[35] C. R. Bingham, J. C. Batchelder, K. Rykaczewski, K. S. Toth, C.-H. Yu, T. N. Ginter, C. J. Gross, R. Grzywacz, M. Karny, S. H. Kim, et al., Phys. Rev. C **59**, R2984 (1999).
[36] T. N. Ginter, J. C. Batchelder, C. R. Bingham, C. J. Gross, R. Grzywacz, J. H. Hamilton, Z. Janas, M. Karny, S. H. Kim, J. F. Mas, et al., Phys. Rev. C **61**, 014308 (1999).
[37] M. Hjorth-Jensen, T. T. S. Kuo, and E. Osnes, Physics Reports **261**, 125 (1995).
[38] R. B. Wiringa, V. G. J. Stoks, and R. Schiavilla, Phys. Rev. C **51**, 38 (1995).
[39] T. Faestermann et al. (2010), presented at the EFES-NSCL Workshop on Perspectives on the Modern Shell Model and Related Experimental Topics, East Lansing, MI.